Tropical Convective Systems

Observed by Infrared Satellite and Radar

National Aeronautics and Space Administration

Goddard Space Flight Center

Greenbelt, MD 20771

Brian D. McNoldy

Submitted on August 15, 1997

Advisor: Thomas M. Rickenbach

TRMM Office, Code 910.1

Section I: Objectives

Since this internship was my first formal exposure to atmospheric science, my objectives were two-fold; personal and scientific. First, my personal objective was to venture out of my undergraduate major area of study, astrophysics, and gain experience in atmospheric science research (particularly convective and squall line systems) in a professional setting. After two and a half months of exhilarating challenges, obstacles, and solutions, I felt both satisfied and motivated to pursue the subject and hope that my academic career will involve the atmosphere, whether it be in the study of extraterrestrial atmospheric dynamics or a more detailed look at mesoscale and synoptic scale convective structures on Earth.

The scientific goals of my brief stay also involved something being done for the first time. After modifying several software routines, I was able to view and analyze the TOGA COARE (Tropical Ocean Global Atmosphere Coupled Ocean Atmosphere Response Experiment) long-range radar scans (out to 295 km). One goal of this experiment was to study the evolution of thunderstorms over the Pacific Ocean. The interaction between convection and the ocean surface in this region (see figure on page 12) influences global weather patterns, such as the El Niño phenomenon. For a much more detailed look at the TOGA COARE project, see Webster and Lukas (1992). The long-range scans are important because they can reveal whether or not there is precipitation under cold (high) clouds over a broad area, where the previously-analyzed shorter-range scans (~120 km) sacrificed this spatial coverage for higher resolution. A closer look at the scientific objectives and their significance will be discussed in *Section II: Results*.

Section II: Results

After converting gigabytes of raw data to useful graphical files that could be printed, I had a chance to look at them and analyze what I had done. In all, I processed 65 hours of data spanning four non-consecutive days (12/24/92, 12/25/92, 2/9/93, and 2/15/93), creating a GIF format image file of horizontal reflectivity maps in the IFA (Intensive Flux Array) at ten minute intervals and at two separate vertical levels (cappis), for a total of 780 gif images. I also made PostScript (ps)

images (better quality for printing) of the reflectivity with infrared contour lines overlaid at two cappi heights per hour, for a total of 110 ps images. The third type of graphical output I created involved two images on one page: the top contains a close-range view of the reflectivity and IR overlay, and on the bottom is the vertical cross section of a slice through interesting features in the reflectivity map. Graphs for this type of output exist at heights of two and ten km and only for six hours on 09feb93 in the IFA, for a total of twelve ps images. There are examples of each of the three kinds of graphs attached to this paper (see pages 16, 17, and 18).

So what does it all mean? The huge volumes of gif files (reflectivity only) will not be discussed in great detail here, they were simply made for future archival/reference purposes and for use in animations. They also serve to study the fine time scale evolution of the convective lines and clusters described in Burgess (1987) and Cotton et al (1989). However, the reflectivity and IR contour overlay maps are very useful. What is reflectivity and how is it found? Reflectivity refers to the amount of the radio pulse reflected back to the emitting radar. If the radio pulse encounters hail or large drops of rain (which are highly reflective due to their large backscatter cross-section), more of the beam will be returned to the radar than if the pulse encounters lighter, smaller rain droplets (which are more effective at scattering the beam). Reflectivity is measured in decibels (dBZ) and is closely related to rainfall rates when drop-size distribution is assumed. Since it is such a fundamental aspect of this project, I will go into detail to explain how it is derived.

Drop-size distribution, rainfall rate, and the reflectivity factor are described in this very basic empirical equation: $Z=AR^b$, where Z is the reflectivity factor, R is the rainfall rate, and A and b are coefficients that are specific to different types of rain (convective and stratiform); they are positive constants obtained from the slopes and intercepts of a logZ vs. logR plot (Houze, 1993). The basic distinction between convective and stratiform rain is the vertical wind velocity relative to the hydrometeor fallspeed in that vicinity. But what about dBZ? It is related to Z in the following way: $dBZ=10 \cdot \log Z$. Finally, dBZ can be related to A, b, and R using the previous equations; $\mathbf{dBZ = 10 \cdot logA + 10b \cdot logR}$. For typical convective features during TOGA COARE, values of A=120 and b=1.43 will be used (Tokay and Short, 1996). Be aware that these coefficients do not apply to mid-latitude convective features. This derivation and declaration of

constants allows us to calculate the rainfall rate from an observed reflectivity. The chart below is a result of such a calculation, using the previously mentioned constants.

TOGA COARE Reflectivity/Rainrate Correspondence

dBZ	mm/h	
50	110.289	(~4" per hr)
45	49.304	
40	22.041	
35	9.853	
30	4.405	
25	1.969	
20	0.880	
15	0.394	
10	0.176	
5	0.079	
0	0.035	
-5	0.016	
-10	0.007	(~1/5000" per hr)

Several periods exhibited features that had a leading edge of convection with a trailing region of stratiform rain (see figure on page 13). The leading edge of convection, called a squall line, typically moved eastward during TOGA COARE. Stratiform rain, or rain falling as a by-product of deep convection, almost always fell westward (downwind) of the squall line and increased in volume after the peak of convection occurred. As noted in Chen et al (1996), ice particles pushed up into the anvil by convection typically fall out after traveling about 300 kilometers downwind from their convective "parents". For a detailed look at the evolution of squall lines and the convective/stratiform relationship, see Heymsfield and Fulton (1994) and Rasmussen and Rutledge (1993).

Rather than occurring in an organized line, convection was sometimes observed to occur in clusters. In fact, non-squall clusters are a more common phenomenon than squall lines, and therefore play a more important role in the overall rainfall climatology (Cotton and Anthes, 1989). A non-squall cluster refers only to the satellite view of a mesoscale system, since it is not well understood what the clusters are in terms of rainfall organization. During a particular clustering event, cells could not be tracked for very long without confusion. The cells and groups of cells interact very dynamically and do not maintain their own identity for more than a couple of hours.

Furthermore, the larger cloud clusters showed appreciable diurnal variation, with a maximum of convective activity at about 0400 and a minimum of activity at about 1700 (Chen et al, 1996). According to Mapes (1993), "cloud clusters merge, split, and mingle so gregariously that it becomes impossible —and perhaps meaningless— to track them as individual entities".

Why does it matter if convection occurs in the form of individual cells, multicellular clusters, or squall lines? One of the big reasons is that the rainrate of a particular precipitating cloud feature is affected by how much surface area is exposed to the relatively dry surrounding environment. First of all, precipitating deep convection depends on the supply of humid air available in the lowest few hundred meters above the ground (Mapes, 1993). Secondly and most importantly, individual cells typically have the lowest rainrates, while clusters (Mesoscale Convective Complexes, or MCC's) generally produce the highest rainrates (Scofield, 1987).

The remainder of this section will focus on the evolution of squall lines (from radar) and the associated cloud mass area and temperature (from IR satellite). When a convective feature develops, its updraft is strong enough to bring clouds and ice particles up to 15 or even 18 km above the ground (remember, the updraft is capable of suspending millions of tons of water above the ground). These cloud tops become very cold and show up quite well on infrared satellite imagery. Some of the coldest cloud tops during TOGA COARE dropped to temperatures of 190K (-92° F). Mapes and Houze (1993) use 188K (-121° F) for the tropopause (troposphere/stratosphere boundary) temperature in the warm pool, 241K (0° F) for the maximum temperature that an MCC can have, and 208K (-60° F) as the temperature corresponding to the location of a mature oceanic mesoscale convective system.

Due to the geometry of a squall line system (a straight line, sometimes warped into an arc or bow), it is not unusual for a gust front to form. A gust front and its associated arc cloud are the result of cold downdrafts rushing out in front of the deepest convection and heaviest precipitation (see figure on page 14). If the gust front is powerful enough, it can act like a mid-latitude cold front, "scooping" warm, humid air up and creating new thunderstorms in its path. This process is demonstrated idealistically during the evening hours of 9feb93 (0700Z - 1100Z). In this case, the squall line produced a gust front, the gust front accelerated ahead, leaving its "parent" squall line

behind to decay, then the gust front eventually became the major squall feature of the day. If the radar data covered more area, a new, "grandchild" gust front might have been observed to form from the dying squall line. This transfer of convective features is important to understand because of its affect on convective available potential energy (CAPE), net heating aloft, and net cooling at the ocean's surface (Webster and Lukas, 1992). This significance of this process will be covered in greater detail later in the paper.

The location of the western Pacific warm pool makes it extremely difficult to obtain radar data. The area of interest is hundreds to thousands of kilometers from land, and shipboard radar (like that used during the three-month period of TOGA COARE) is expensive to organize and maintain. So what other options exist to determine how much precipitation is falling in a given location? As mentioned earlier, quite a bit of information can be obtained via infrared satellite. In the absence of radar data, precipitating clouds must be inferred from cloud types and their evolution (Scofield, 1987). By knowing the temperature of a cloud top, the height of the cloud can be derived (seasonal and geographic factors complicate this derivation), and once the height is known, the strength and size of the main updraft can be deduced, and finally, the type and amount of precipitation is dependent on the details of the updraft. Understanding the underlying structure of the anvil is crucial to be able to deduce what type and how much precipitation is occurring. According to Chen et al (1996), large-scale tropical convection is intimately related to the fine precipitation structure of convective systems.

The study of the formation, evolution, and decay of convective anvils can, in the long term, be an important tool in the prediction of global weather patterns. The reasoning of this previous statement will be discussed later in the paper. Anvil morphology is not only important, but it can be observed rather easily since IR satellites pass over any given location on the globe several times daily. The anvil is only formed after the convection has had enough time to push ice particles up to that altitude (~15-18km). However, Zipser (1988) mentions that severe weather (and thus the heaviest precipitation) is strongly associated with the organizing stage and is less common once the cold cloud area reaches a maximum (see figure on page 15). Although anvils are huge formations, they account for only 10% of the total area of tropical disturbance cloud cover because of their

relative rarity (Johnson, 1984). It is important to distinguish between increasing areal coverage of the anvil and increasing areal coverage of the coldest parts of the anvil. Strong winds aloft are responsible for spreading the entire anvil; however, expansion of the coldest temperatures is the indicator of convective intensity. Furthermore, clouds with cold expanding coverage produce more rainfall than those not expanding, and the more rapid the expansion of the coldest tops, the heavier the rainfall (Scofield, 1987). It should also be noted that the coldest temperatures always occur slightly downwind from the deepest convection (due to wind shear), even during the peak of activity.

Now the basics of anvil creation have been covered, but how does one go about using anvil morphology to decide what is occurring under the immense shield of ice? Fortunately, most cases during TOGA COARE showed an evolution dependence, that is, increasing anvil displacement with increasing time (Heymsfield and Fulton, 1994). The key element in this is the fact that low-level winds were westerly (W-E), while upper-level winds were easterly (E-W). Since the vast majority of the system's mass lies close to the ground, the main convective line tracks eastward; however, the lighter upper portions of the cloud are influenced by the easterlies and are dragged westward. Zipser (1988) observed that the coldest cloud tops shift away from convective and towards stratiform and eventually break away with time. These detached anvils can last for longer than half a day, just drifting westward. As one would expect, the visual difference between a "living" and a "dead" anvil is not very great. Rickenbach et al (1997) points out that the advection of cold anvils away from their convective sources complicates the interpretation of system motion and structure.

One method does exist for determining the relationship between anvil growth and underlying convection. Both Rickenbach et al (1997) and Scofield (1987) supply an insight regarding anvil evolution and temperature changes. Scofield states that the warmer parts of the anvil continue to spread long after vertical motion has ceased, giving the appearance that the storm is growing in size... this is not the case (only the cloud is expanding, not the storm itself). Rickenbach et al expands on this idea and describes the temperature/convection relationship. Infrared temperature ($T_b \equiv$ brightness temp.) "features are intimately linked to the life cycle of the

convective source". When convection is deepest, huge amounts of ice are pushed up into the upper troposphere, resulting in cold cloud tops. When the convection weakens, the ice particles start to fall and at the same time, get blown downwind by strong upper-level winds. The end product (after several hours) is an anvil whose coldest T_b features gradually warm and spread out horizontally. This is the process to monitor that signifies the detachment of the anvil from the convective source; areal coverage of cold T_bs decreases, areal coverage of warm T_bs increases, and the entire anvil expands horizontally (primarily downwind), and finally, the dead anvil stops moving eastward and begins to drift westward. The entire process described above was observed on several occurrences during the four days that I processed and analyzed.

Finally, the long-term goals of learning about precipitation from infrared satellite measurements will now be discussed. As mentioned in *Section I: Objectives*, Webster and Lukas (1992) provide an in-depth look at TOGA COARE and its implications for the future of planetary-scale weather forecasting; however, I will summarize the big issues relevant to this paper for the comfort of the reader (Webster and Lukas is forty pages long). Precipitation, which transfers moisture from the atmosphere to the ocean, may impact the dynamics of the warm pool. How? Heavy rains create a freshwater "lens" on the top few meters of the ocean. This lens both insulates the cool water below and readily absorbs heat provided by the sun (low salinity allows for higher temperatures; high salinity keeps the temperature lower). The exact location, size, and depth of this lens is important because the tropical atmosphere is sensitive to small variations in sea surface temperature (SST). Furthermore, SST also affects the ocean's CO_2 absorption capacity. Alterations in the SST could lead to dramatic changes in global circulation, tropical cyclone development, and the El Niño Southern Oscillation (ENSO).

Section III: Methods Used to Achieve Results

First and foremost, it is important —if not essential— to bang one's head on one's desk repeatedly during troublesome times. More specifically though, the results and analysis discussed in *Section II: Results* were all accomplished by the use of six main programs (three in C and three

in IDL). Before using any program however, the raw data collected during TOGA COARE was retrieved off of 8mm tapes and temporarily stored on a workstation (trmm).

Then, the first C program (tc2cap) was run to convert the "Universal Format" data into a radar cappi structure. Next, tc_cap2cart was run to convert the polar cappi output from tc2cap to a cappi structure mapped onto a cartesian plane. This conversion explains why the previous analysis only used reflectivity information out to 120km; the further out one goes from the radar, the more the data points get stretched and distorted to compensate for the change in coordinate systems. Each of the previous two programs needed to be run for both radars (MIT and TOGA) and at two cappi heights (2 and 4 km); this process was by far the most time-consuming aspect of data manipulation. The final C program is merge_dbz which merges the reflectivity maps from both radars at a given time. This needed to be run at two cappi heights as well. Although not recognized in the *Acknowledgments* (page 22), I will take this opportunity to thank Paul Kucera, author of the three C programs and their associated sub-routines. All that remained for me to do (tricky as it was) was to reconfigure the programs to create a larger data array and to alter the reflectivity bounds and rainrates.

Visualization of the data was now ready to take place. This was done with three IDL routines. These programs are not nearly as complicated or cryptic, and are very flexible as far as the output options are concerned. Brief descriptions of each of these can be found in *Section IV: Data Storage*. The only one that might need a little more explanation is the third one (cappi_ir_rhi_DATE_TIME.pro; the output is on page 18). The top half shows a detail of the horizontal reflectivity map (at 2km or at 10km) with a thin black line drawn through it. This thin line marks the location of the vertical cross section which is shown in the bottom half. The line is purposely chosen to run through interesting features (usually deep convection) and can be relocated for any other time. This technique is extremely important when analyzing the area of deepest convection, the trailing stratiform region, and the morphology of the precipitating sections of the anvil.

Once the software routines were finished, the remainder of the analysis was subjective, using nothing more than the human eye to locate potentially interesting convective features and

then decide what was physically occurring. Having the reflectivity map at two heights, the IR contour overlays, and the vertical cross section, the internal processes of the system could be estimated, and finally, the overall structure of the storm could be deduced.

Section IV: Data Storage

Raw (Universal Format) data from all three cruises during TOGA COARE are on 8mm data tapes, and are labeled with the dates and times contained on each tape.

The output from tc2cap.c is on trmm; /data1/mcnoldy/DATE/tc2cap_out/. The files have the format tog_930209_0600.cap.uf.gz, where tog could be mit, and the dates and times will vary (see attached program description on page 19 for details). These files exist from 0300Z to 2350Z on 24dec92, from 0000Z to 1200Z on 25dec92, from 0600Z to 1800Z on 9feb93, and from 0000Z to 2000Z on 15feb93.

The output from tc_cap2cart.c is on trmm; /data1/mcnoldy/DATE/cap2cart_out/. The files have the format tog_930209_0600_dbz_2.0km.img.gz, where tog could be mit, and the dates and times will vary and the cappi heights that exist are 2.0 and 4.0 km (see attached program description on page 20 for details). These files exist for the same time intervals and dates as tc2cap.c.

The output from merge_dbz.c is on trmm; /data1/mcnoldy/DATE/merge_out/. The files have the format mit_tog_930209_0600_dbz_2.0km.img.gz, where the dates and times will vary and the cappi heights that exist are 2.0 and 4.0 km (see attached program description on page 21 for details). These files exist for the same time intervals and dates as tc2cap.c.

The output from dbzimage_map_ifa_binary.pro is on trmm; /data1/mcnoldy/DATE/HEIGHT/gif/. This program is currently set up to produce a landscape-oriented gif file of the reflectivity only using the output from merge_dbz.c. The files have the format rain_dbz_020993_0600.gif, where the dates and times will vary, and the possible height directories are 2.0 and 4.0. These files exist for the same time intervals and dates as tc2cap.c.

The output from rain_ir_overlay_binary.pro is on trmm; /data1/mcnoldy/DATE/HEIGHT/ps/. This program is currently set up to produce a landscape-oriented ps file of the

reflectivity with IR contours overlaid, using the output from merge_dbz.c. The files have the format rain_ir_9feb93_0600.ps, where the dates and times will vary, and the possible height directories are 2.0 and 4.0. The files exist from 0340Z to 2340Z on 24dec92, from 0040Z to 1140Z on 25dec92, from 0640Z to 1540Z on 9feb93, and from 0240Z to 1545Z on 15feb93.

The output from cappi_ir_rhi_DATE_TIME.pro is on trmm; /data1/mcnoldy/DATE/ volumes/ps/. This program is currently set up to produce a portrait-oriented ps file of the IR contours/reflectivity on the top half, and a vertical cross section in the bottom half. The location of the input is mentioned in the program itself. The output files have the format ir_cappi_2km_9feb93_0942.ps, where the dates and times will vary, and the possible heights are 2km and 10km. The files exist from 0942Z to 1442Z on 9feb93.

Section V: References

Burgess, D. W., and L. R. Lemon, 1987: Severe Thunderstorm Detection by Radar. *Radar in Meteorology*, Chapter 30a. American Meteorological Society, Boston, MA, 619-647.

Chen, S. S., R. A. Houze, Jr., and B. E. Mapes, 1996: Multiscale Variability of Deep Convection in Relation to Large-Scale Circulation in TOGA COARE. *Journal of the Atmospheric Sciences*, **53**, 1380-1409.

Cotton, W. R., M. Lin, R. L. McAnelly, and C. J. Tremback, 1989: A Composite Model of Mesoscale Convective Complexes. *Monthly Weather Review*, **117**, 765-783.

——, and R. A. Anthes, 1989: *Storm and Cloud Dynamics*. Academic Press, 595-612.

Heymsfield, G. M., and R. Fulton, 1994: Passive Microwave and Infrared Structure of Mesoscale Convective Systems. *Meteorology and Atmospheric Physics*, **54**, 123-139.

Houze, R. A., Jr., 1993: *Cloud Dynamics*. Academic Press, 112-113.

Johnson, R. H., 1984: Partitioning Tropical Heat and Moisture Budgets into Cumulus and Mesoscale Components: Implications for Cumulus Parametrization. *Monthly Weather Review*, **112**, 1590-1601.

Mapes, B. E., and R. A. Houze Jr., 1993: Cloud Clusters and Superclusters over the Oceanic Warm Pool. *Monthly Weather Review*, **121**, 1398-1415.

——, 1993: Gregarious Tropical Convection. *Journal of the Atmospheric Sciences*, **50**, 2026-2037.

Rasmussen, E. N., and S. A. Rutledge, 1993: Evolution of Quasi-Two-Dimensional Squall Lines. Part I: Kinematic and Reflectivity Structure. *Journal of the Atmospheric Sciences*, **50**, 2584-2606.

Rickenbach, T. M., D. A. Short, and O. W. Thiele, 1997: Propagation Characteristics of Tropical Convective Systems from Radar and Infrared Satellite Images. *American Meteorological Society: 28th Conference on Radar Meteorology*, Austin, TX, submitted.

Scofield, R. A., 1987: The NESDIS Operational Convective Precipitation Estimation Technique. *Monthly Weather Review*, **115**, 1773-1792.

Tokay, A., and D. A. Short, 1996: Evidence from Tropical Raindrop Spectra of the Origin of Rain from Stratiform Versus Convective Clouds. *Journal of Applied Meteorology*, **35**, 355-371.

Webster, P. J., and R. Lukas, 1992: TOGA COARE: The Coupled Ocean-Atmosphere Response Experiment. *Bulletin American Meteorological Society*, **73**, 1377-1416.

Zipser, E. J., 1988: The Evolution of Mesoscale Convective Systems: Evidence from Radar and Satellite Observations. *Tropical Rainfall Measurements*. Deepak Publishing, 159-166.

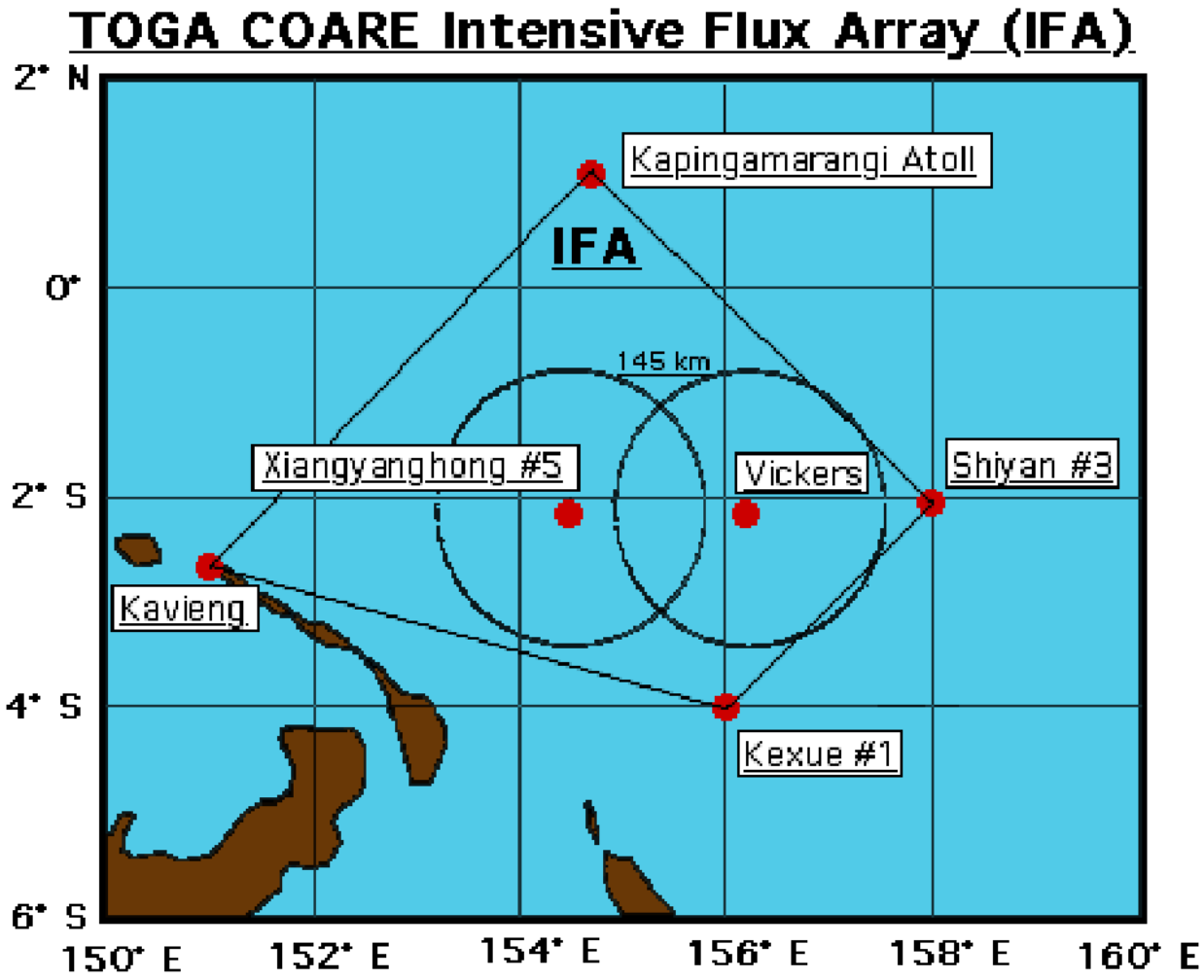

The TOGA radar was on the Xiangyanhong #5, the MIT radar was on the R.V. Vickers. The entire TOGA COARE program lasted from November 5, 1992 to February 22, 1993 (spread out between three cruises, with a one-week break between cruises).

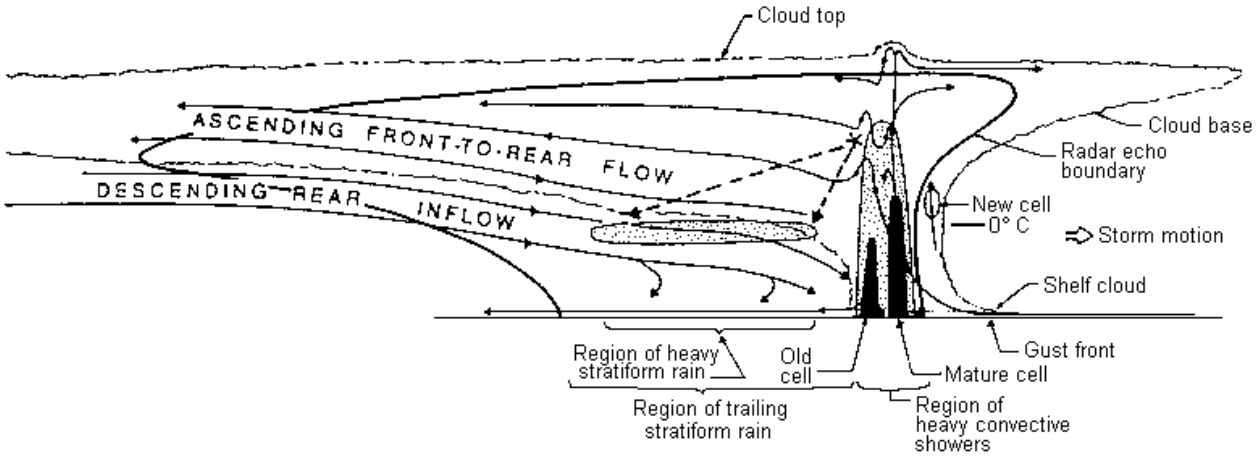

Conceptual model of a squall line with a trailing stratiform area viewed in vertical cross section oriented perpendicular to the convective line (parallel to its motion).
Adapted from Rasmussen and Rutledge (1993).

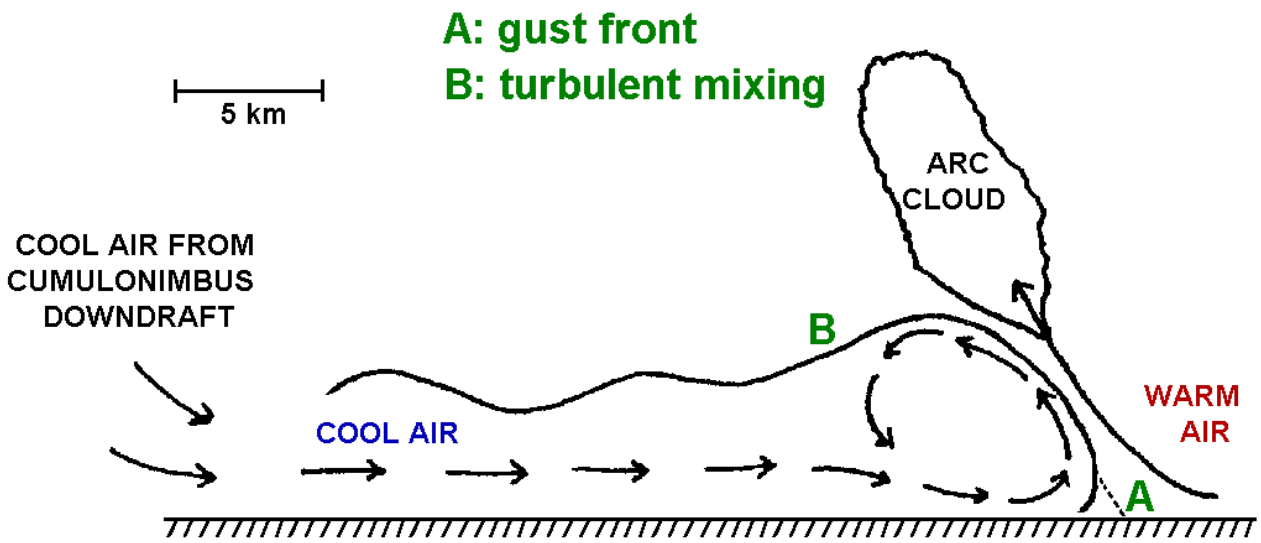

Schematic cross section through the gust front of a thunderstorm.
Adapted from Houze (1993).

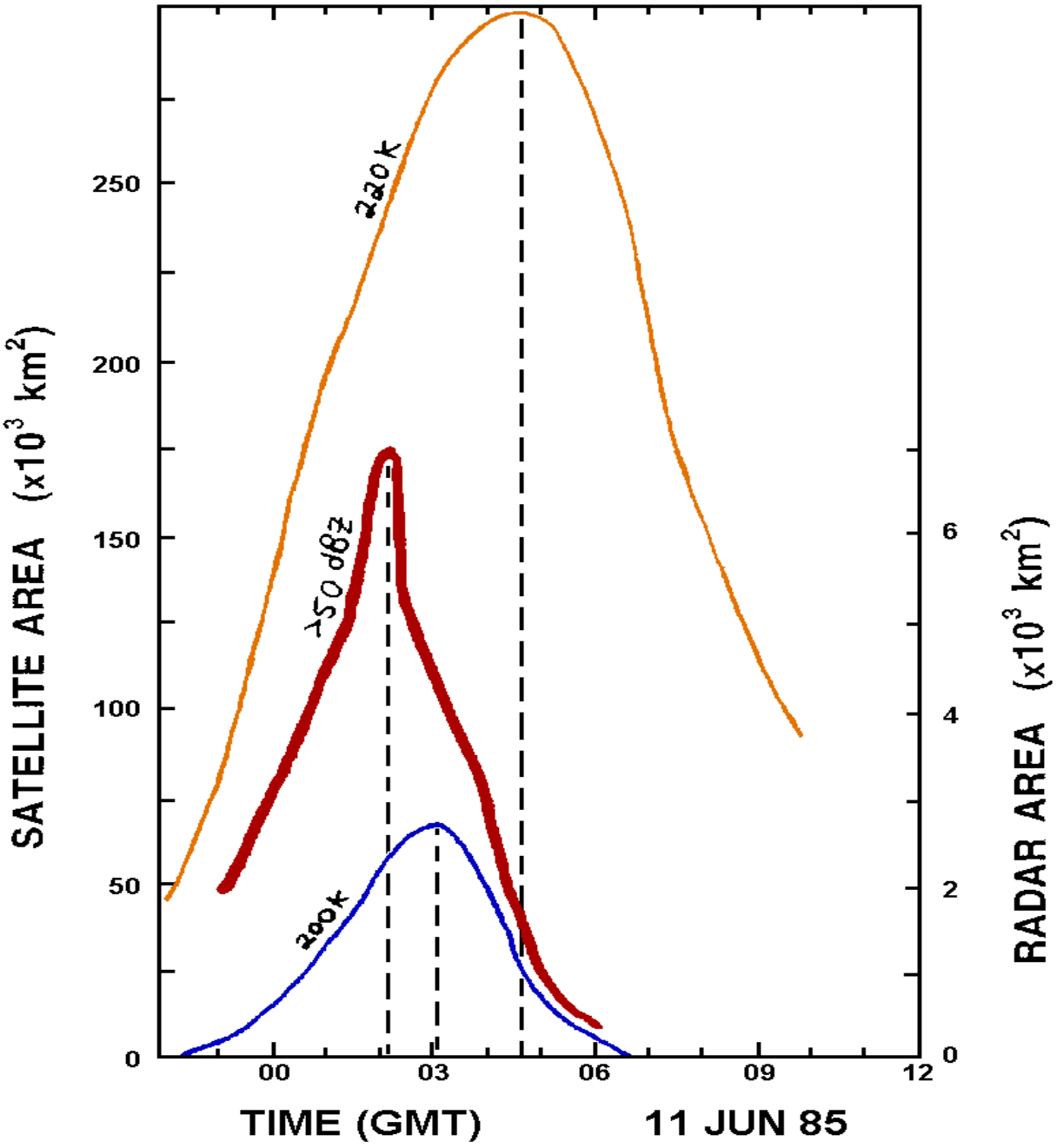

Time variation of area covered by IR temperatures colder than indicated values in a large squall line system over Kansas and Oklahoma.
Adapted from Zipser (1988).

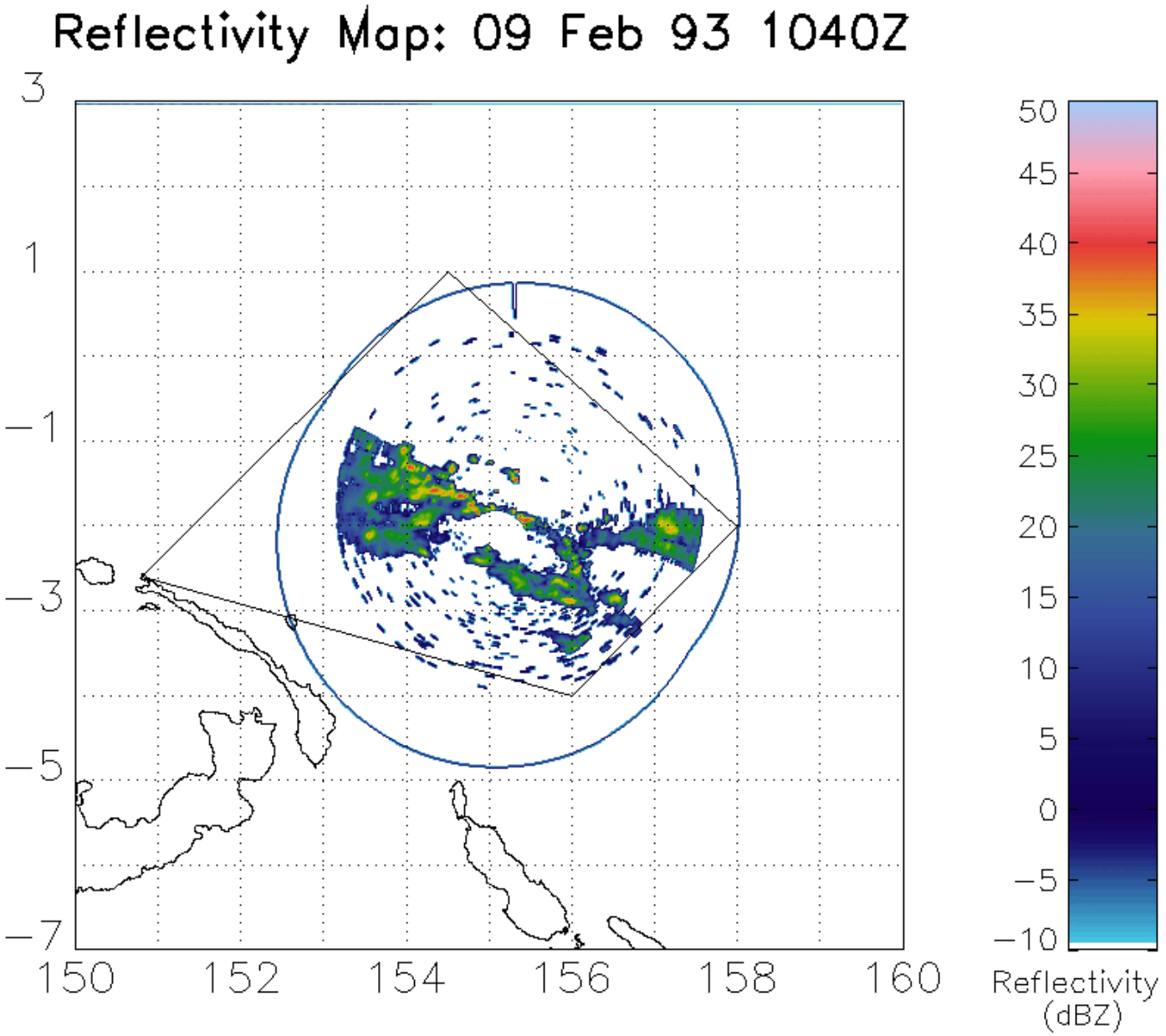
Reflectivity Map: 09 Feb 93 1040Z
3
1
−1
−3
−5
−7
150
152
154
156
158
160
50
45
40
35
30
25
20
15
10
5
0
−5
−10
Reflectivity
(dBZ)

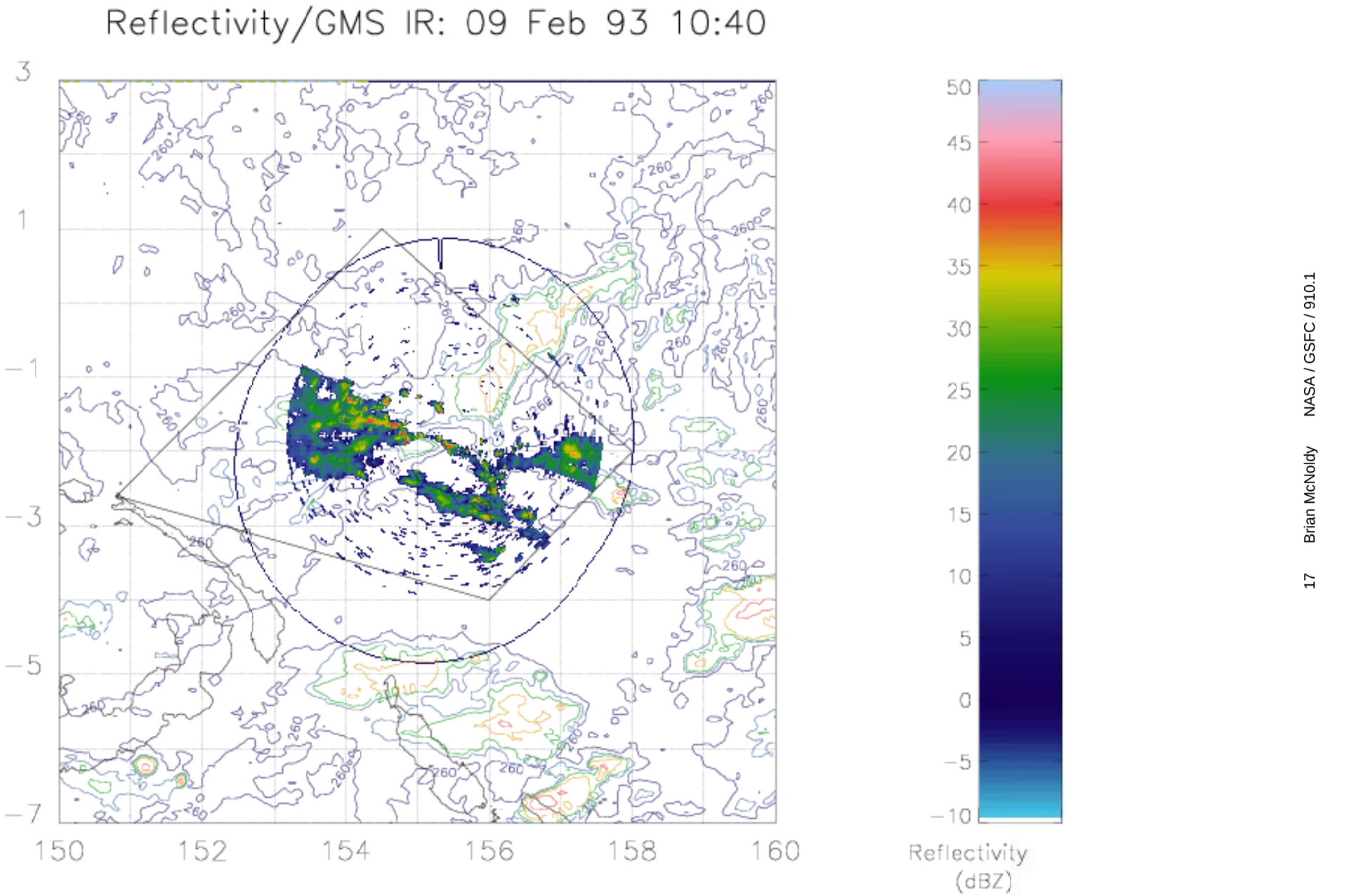

17 Brian McNoldy NASA / GSFC / 910.1

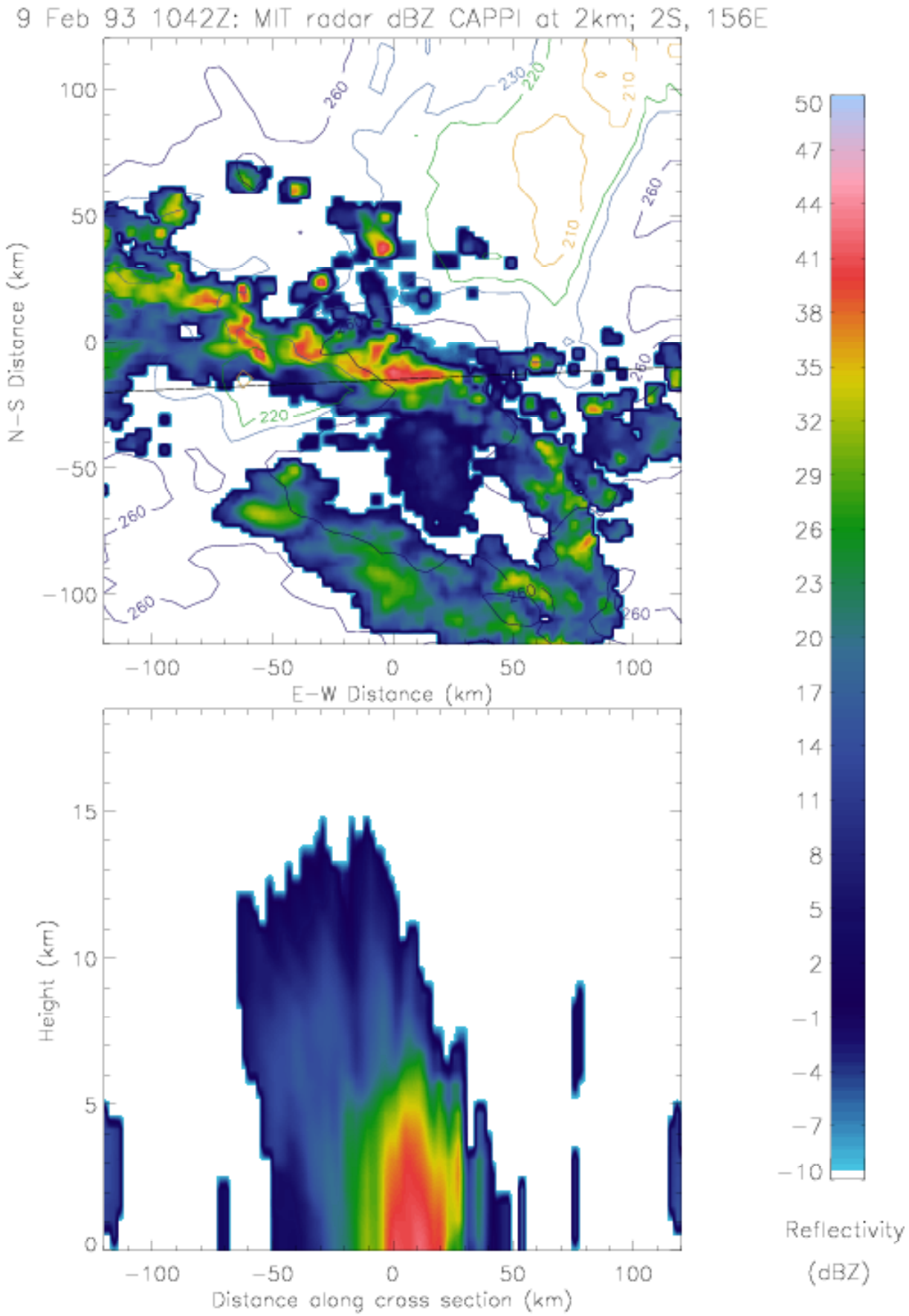
9 Feb 93 1042Z: MIT radar dBZ CAPPI at 2km; 2S, 156E
N-S Distance (km)
E-W Distance (km)
Height (km)
Distance along cross section (km)
Reflectivity (dBZ)
50
47
44
41
38
35
32
29
26
23
20
17
14
11
8
5
2
−1
−4
−7
−10

TC2CAP

Program : tc2cap.c

Location : /user/mcnoldy/radar/tc/tom/

Purpose : Converts compressed, raw, Universal Format (UF) data to a multi-cappi structure that includes reflectivity and echo-top height fields.

General usage :

tc2cap -I *infile* -r *radar* -F *field* [-I *indir*] [-O *outdir*]
[-h *hgt_cap* -H *hgt_file*] [-g] [-G *gifdir*] [-S *sw_lvl*]

Required :

i	input filename
r	radar name {mit=MIT, tog=TOGA}
h	height in for one level cappi
H	height file for multiple level cappis
F	field to analyze {dz, cz}

Optional :

I	input file directory
O	output file directory
g	create gif images of cappi levels
G	send gif file to directory
S	create spectral width at sw_lvl

Example input :

tc2cap -I toga_930209_1140.uf.Z -r tog -F dz -I /data5/mcnoldy/9feb/
-O /user/mcnoldy/9feb -H hgt_lvl.inf

Example output :

the program created a file *tog_930209_1140.cap.uf.gz*
in */user/mcnoldy/9feb/020993/*

TC_CAP2CART

Program : tc_cap2cart.c

Location : /user/mcnoldy/cappi/tc/cart/tom/

Purpose : Converts polar cappi output from tc2cap to a cartesian reflectivity map using the nearest neighbor average scheme.

General usage :

tc_cap2cart -I *infile* -r *radar* -H *img_height* -W *img_width* -p *pix_res* [-l *lvl* -L *lvl_file*] [-h] [-I *indir*] [-F] [-O *outdir*] [-w *weight*]

Required :

i	input filename
r	radar name {mit=MIT, tog=TOGA}
H	height (y) of image in pixels
W	width (x) of image in pixels
p	pixel resolution in km
l	height to create dBZ image in km
L	heights to create dBZ images from lvl_file

Optional :

I	input file directory
O	output file directory
h	write header of HEADER_SIZE to file
w	number of sub-grid points to average
F	create ASCII output

Example input :

tc_cap2cart -I tog_930209_1140.cap.uf.gz -r tog -H 556 -W 556 -p 2 -L hgt_lvl.inf -h -I /user/mcnoldy/9feb/020993/ -O /user/mcnoldy/9feb

Example output :

the program created a file *tog_930209_1140_dbz_2.0km.img.gz* in */user/mcnoldy/9feb/2.0/020993/* and a file *tog_930209_1140_dbz_4.0km.img.gz* in */user/mcnoldy/9feb/4.0/020993/*

MERGE_DBZ

Program : merge_dbz.c

Location : /user/mcnoldy/cappi/tc/merge/

Purpose : Combines the multi-level cartesian reflectivity maps from tc_cap2cart into a single cartesian reflectivity map.

General usage :

merge_dbz -[vpawmC] -b *begin_date* -s *start_hr* -e *end_date* -f *finish_hr* -I *merge_dir* -M *mit_indir* -T *tog_indir* -L *hgt_file*

Required :

b	beginning date
s	starting hour
e	ending date
f	finishing hour
I	output directory for merged images
M	MIT radar input directory
T	TOGA radar input directory
L	height levels to process (ascii file)

Optional :

v	Vickers dominant
p	PRC (Xiangyanhong) #5 dominant
a	average data in common area
w	range weighted average in common area
m	use max value in common area
C	files are compressed (gzip)

Example input :

merge_dbz -m -b 930209 -s 0600 -e 930209 -f 1300 -I /user/mcnoldy /9feb/merge -M /user/mcnoldy/9feb -T /user/mcnoldy/9feb –L hgt_lvl.inf

Example output :

the program created a file *mit_tog_930209_0600_dbz_2.0km.img* (0600,0610,...,1350) in */user/mcnoldy/9feb/merge/2.0/020993/* and a file *mit_tog_930209_0600_dbz_4.0km.img* (0600,0610, ...,1350) in */user/mcnoldy/9feb/4.0/020993/*

Acknowledgments:

The following people helped to make this experience

- possible,

- more enjoyable,

- more comfortable

- more informative,

- more friendly:

● **Tom Rickenbach** ● **Per Gloersen**

♦ Richard Bosley ■ Richard Erickson ● Brad Fisher

■ David Fisher ● David Makofski ♦ Harry Sheets

● David Short ● Joanne Simpson ♦ Hazel Stephenson

● Otto Thiele ● Ali Tokay

■ David Wolfe ● David Wolff

●= **GSFC** ♦ =**UMCP** ■=**Lycoming College**

And of course, my family and friends.

.